Heliyon 9 (2023) e16277

Contents lists available at ScienceDirect

Heliyon

journal homepage: www.cell.com/heliyon

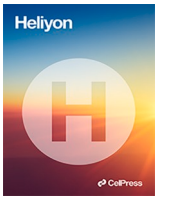

Research article

Eco-friendly green synthesis of silver nanoparticles from *Aegle marmelos* leaf extract and their antimicrobial, antioxidant, anticancer and photocatalytic degradation activity

P. Rama [a], P. Mariselvi [b], R. Sundaram [c], K. Muthu [a,*]

[a] *Department of Chemistry, Manonmaniam Sundaranar University, Abishekapatti, Tirunelveli, 627012, Tamil Nadu, India*
[b] *Department of Chemistry, Rani Anna Govt. College for Women (Affiliated to Manonmaniam Sundaranar University, Tirunelveli, 627012, Tamil Nadu, India), Tirunelveli, 627008, Tamil Nadu, India*
[c] *Department of Biochemistry, Saveetha Dental College & Hospital, Saveetha Institute of Medical & Technical Sciences, (Saveetha University) Vellapanchavadi, Chennai, 600077, Tamil Nadu, India*

ARTICLE INFO

Keywords:
Aegle marmelos
Silver nanoparticles
MDA-MB-231
Cytotoxicity
Photocatalyst

ABSTRACT

The present research work, green synthesis of silver nanoparticles (Ag NPs) was synthesized from silver ions using the reducing and capping agents of *Aegle marmelos* leaf extract. Initially, UV–vis spectrophotometry absorption of the Surface Plasmon Resonance centre at 450 nm was confirmed the formation of Ag NPs. Preliminary phytochemical and FT-IR analysis indicate the identification of secondary metabolised flavonoids that act as the reducing and capping agent of the synthesized Ag NPs. Transmission electron microscope analysis, morphology of Ag NPs shown by transmission electron microscopy is spherical with a size range of ~30–50 nm. The synthesized Ag NPs were investigate the *in-vitro* anticancer, antimicrobial and antioxidant activity, results shows the potential activity against the standard drugs. The Ag NPs also revealed the cytotoxicity against MDA-MB-231 human breast cancer cells. The MTT assay shows the IC_{50} values at 125 ± 4.26 μg/mL of Ag NPs compared to the untreated cells of negative control. The Ag NPs was excellent photocatalyst act as degradation of environmentally polluted Basic Fuchsin dye within 18 min.

1. Introduction

Cancer is the most widespread disease on earth that is uncontrollable by our human body's cells. In particular, Breast cancer was the second most common malignant tumor, affecting mainly women and causing deaths worldwide [1]. Several categories of cancers can be identified. Chemotherapy is one of the standard treatment to improve the healthy cell [2–4]. Recently, the phenomenal growth of nanotechnology has ushered in a new era in materials research for significant applications in Physico-chemical science, biological science, nanotechnology, electronics, medicine, catalysis, optics, and bioengineering [5]. Among the noble metallic nanoparticles, silver nanoparticles (Ag NPs) have gained popularity in recent years due to their numerous applications, such as antioxidant, antibacterial, anti-angiogenic, wound healing, anti-inflammatory, anticancer activity [6]. Among the several metals, silver was gaining popularity due to its well-known medicinal properties [7]. Now-a-days medicinal plant extract mediated synthesis of Ag NPs shows the therapeutic applications [8]. Specifically, *Piper nigrum* seed [9], *Bergenia ligulata* (whole plant) [10], *Leucas biflora* (Vahl) Sm. leaf [11],

* Corresponding author.
E-mail address: karu.muthu@msuniv.ac.in (K. Muthu).

https://doi.org/10.1016/j.heliyon.2023.e16277
Received 29 December 2022; Received in revised form 8 May 2023; Accepted 11 May 2023
Available online 18 May 2023

Abutilon indicum leaves [12], *Scutellaria multicaulis* stem [13], and *Baccaurea ramiflora* (Latka) Juice [14] extracts used in the green/biosynthesis of Ag NPs shows the potential biological therapeutic remedies especially antioxidant, antimicrobial and anticancer activity.

Organic dyes are mostly used in textiles, paint, paper, leather, food, plastics, cosmetics, pharmaceuticals industries etc. [15,16]. These industries, which dump dye waste straight into the water, have emerged as a major contributor to pollution in the global environment [17,18]. Every year approximately 700 million kg of the wastewater dyes are being discharge to land, soil, and air [19]. The dye wastewater had a significant impact on our human and animal bodies, as well as the plant kingdoms. Recently, several physic-chemical and biological techniques such as physical adsorption, electrochemical oxidation, photodegradation, reverse osmosis, catalytic wet oxidation, biodegradation, and chemical reduction methods has been developed to removal of waste dye [20–22]. Few approaches were used to degrade or reduce the waste dyes are economically high and larger procedure to get a lower energy efficient output. Among biosynthesized MNPs employed, as an attractive catalyst in the reduction/degradation of wastewater dyes seems to have a cost-effective and energy-efficient method.

Aegle marmelos L., (*A. marmelos*) also known as bael (bili or bhel, Bengal quince, golden apple, Japanese bitter orange, stone apple, or wood apple) belongs to the Rutaceae family. *A. marmelos* is used as a therapeutic plant in India's traditional system of medicine, Ayurveda. Moreover, its various parts are used to treat a variety of ailments. It checks glucose levels and aids in the maintenance of healthy digestive tracts. Bael has many advantages and uses, for example to fix tuberculosis, diarrheal, clogging, helpful in worm pervasion and stomach-related issues. It contains tannic corrosive, unpredictable oil, adhesive fluid, and polyphenols alkaloids, terpenoids, and phenylpropanoids that help in the decrease of the metal [23,24]. *A. marmelos* plant has a natural healing capacity as well as anti-inflammatory, antipyretic, anti-diarrhoeal, anti-diabetic, analgesic, antimicrobial, radio protective, anticancer, and antiviral properties in various parts [25]. A diverse range of bioactive molecules produced by plants is a rich source of different types of medications. Nowadays, most drugs are obtained from natural sources or semi-synthetic derivatives of natural products, which are mostly used in traditional systems of medicine [26]. Although the literature has reported on the strong medicinal potential of the various parts of *A. marmelos* leaf extract, there is no available data in the literature for the green fabrication of *A. marmelos* leaf extract-mediated Ag NPs that a biocompatible and cost-effective surface-bioactive agent for cancer cells. Therefore, this study was design to fabricate Ag NPs using a biological system and evaluate potential toxicity and the general mechanism of biologically synthesized Ag NPs in MDA-MB-231 human breast cancer cells.

2. Materials and methods

2.1. Collection of A. marmelos and its extraction method

The chosen, healthy and naturally grown *A. marmelos* leaf plants were collected in Tirunelveli district, Tamil Nadu, India. Herbarium specimens were gathered, and their taxonomic identity was verified by Dr. M. Uthayakumar, a taxonomist and assistant professor in the department of plant science at Manonmaniam Sundaranar University in Tirunelveli-12. *A. marmelos* leaves were collected locally, cleaned thoroughly with running tap water and then Milli-Q water to eliminate all visible contamination, chopped into tiny pieces, and dried at room temperature. About 10 g of the leaf were taken in the 250 mL Erlenmeyer flask and added 100 mL deionized water then boiled for 30 min at 80 °C. The unwanted material was filtered out with the help of Whatmann No.1 filter paper. The filtrate (yellow colour) was collected and used for further studies.

2.2. Green synthesis of Ag NPs from silver ions

About 15 mL of 1 mM solution silver nitrate was taken in a 50 mL conical flask and 1 mL of *A. marmelos* leaf extract was added dropwise. The reaction mixture's colour changes from colourless to yellowish brown indicating the product formation of Ag NPs. The formation of Ag NPs was periodically monitored by UV–Vis spectroscopy at different time intervals. The product Ag NPs was separated by triplicate centrifugation at 8000 rpm for about 20 min and washed with deionized water. The obtained residue was dried in a vacuum oven at 70 °C for 6 h. Finally, the obtained powder was collected and stored in a refrigerator for further use [27].

2.3. Characterization of synthesized Ag NPs

The synthesized Ag NPs were periodically characterized by various spectral techniques. The Ag NPs were recorded using LAMBDA XLS, PerkinElmer model UV–vis. spectrophotometer between 200 and 800 nm. XRD data were recorded by ECO D8 Advance elemental composition analyzer (Brucker). The functional group responsible for the Ag NPs was also analyzed by FT-IR (Thermo Scientific Nicolet IS5 Spectrometer) in the wave number range 4000–400 cm^{-1} and the morphology of Ag NPs was shown in a transmission electron microscope (JOEL JEM 21200).

2.4. Antimicrobial activity

The well diffusion method was performed on Muller Hinton agar with selected different concentrations (5, 10, and 25 μg/mL) of Ag NPs and *A. marmelos,* leaf extract was evaluated for antimicrobial activity [28]. The activity was tested against Gram-positive bacteria (*S.aureus, Streptococcus Sp*), Gram-negative bacteria (*Klebsiella Sp, P. aeruginosa*), and fungal strains (*A.niger, Candida Sp, A. flavus, and Penicillium Sp*) with Chloramphenicol and Nystatin as a positive control. At 30 °C, the plates were incubated for 24–72 h. Following an

incubation time, the zone of inhibition around the well was measured.

2.5. Antioxidant analysis

The method was performed according to the M.S. Blois, with slight modification [29]. An aliquot of different concentrations of *A. marmelos* leaf extract and Ag NPs (25–500 μg/mL) and 1 mL of methanol were mixed with 2.5 mL of 0.5 mM DPPH in methanol and the mixture was allowed to incubate in the darkroom for half an hour. At 517 nm, the absorption was measured by a UV–vis spectrophotometer. A blank and ascorbic acid of DPPH-methanol reagent without a sample is utilized to control. Each concentrate experiment is repeated at least three times. The below equation shows the scavenging activity which is calculated as a percentage applied.

$$\text{DPPH scavenging activity (effect \% inhibition)} = \left[\left(A\_(0) - A\_(1)\right)\right] / A\_(0)\ ] \times 100$$

2.6. Anticancer activity of Ag NPs against MDA-MB-231 cell line

The Human Breast cancer cell line (MDA-MB-231) were plated separately using 96 well plates with the concentration of (1×10^4 cells/well) in DMEM media with 1X Antibiotic Antimycotic solution and 10% fetal bovine serum (Himedia, India) in a CO_2 incubator at 37 °C with 5% CO_2. The cells were washed with 200 μl of 1X PBS, and then cells were treated with different concentrations of Ag NPs and *A. marmelos* leaf extract (25, 50,100,250, and 500 μg/mL). The plate system was replaced in an incubator for 24 h. After incubation, MTT solution was added to each and every well. The plate was kept under dark conditions inside the incubator at 37 °C for 4 h on CO_2 incubator. After 4 h, the supernatant content was removed and the purple-blue colour formation was diluted by adding 100 μL of DMSO. The absorbance was measured at 570 nm using a microplate reader. The cytotoxicity index was determined using the untreated cells as negative control. The optical density was used to calculate the percentage of cell cytotoxicity [30].

$$\text{\% Cell viability} = (\text{OD value for test} \ / \ \text{OD value for control}) \times 100$$

$$\text{\% cytotoxicity} = 100 - \text{\% cell viability}$$

2.7. Photocatalytic degradation of Basic Fuchsin dye

The synthesized Ag NPs were used as photocatalyst in the degradation of environmentally polluted Basic Fuchsin (BF) dye. About 1 mL of the catalyst (Ag NPs) was added into the 25 mL of dye solution (25 mg/L). The reaction mixture was irradiated direct solar light. During irradiation time, 3 mL of reaction mixture was taken in quartz cuvette and recorded to the UV–vis spectrophotometer in the wavelength range 200–800 nm at different time intervals.

3. Results and discussion

3.1. UV–vis spectroscopy analysis of green synthesized Ag NPs

Green synthesis of Ag NPs was synthesized from 15 mL of 1 mM silver nitrate solution in the presence of 1 mL of *A. marmelos* leaf

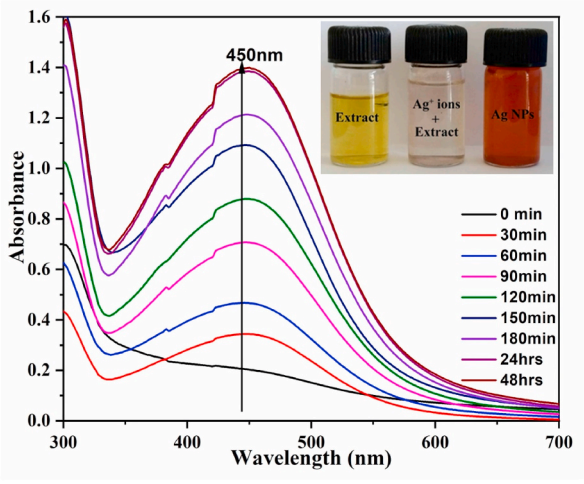

Fig. 1. UV–Vis spectroscopy of the green synthesized Ag NPs at different time intervals and insert image is colour change the formation. (For interpretation of the references to colour in this figure legend, the reader is referred to the Web version of this article.)

extract. The creation of Ag NPs was visually observed by the appearance of yellowish-brown (Insert Fig. 1) colour respectively in the reaction mixture [27]. The appearance of UV–vis spectroscopy surface Plasmon resonance (SPR) absorption peak at 450 nm (Fig. 1) were confirmed the formation of Ag NPs. The conversion of Ag NPs was periodically recorded by UV–Vis spectra at different time intervals. After 48 h, the absorbance intensity level difference was very slight. Therefore, to conclude the maximum amount of silver ions was reduced to Ag NPs. The SPR patterns and characteristics of Ag NPs strongly depend on particle size, stabilizing molecules or the surface adsorbed particles, and the dielectric constant of the medium [31].

3.2. FT-IR analysis

FT-IR analysis determined the phytochemicals present in the *A. marmelos* leaf extract and synthesized Ag NPs as shown Fig. 2a. The wave number value at 3360 and 3439 cm^{-1} was assigned as –OH stretching band in alcohols/phenolic compounds with strong hydrogen bonds or the –NH stretching band of amino groups [27,32]. The absorption band at 2900 cm^{-1} can be related to –CH stretching vibrations and the observed band at 1626 and 1653 cm^{-1} was suggesting the presence of carboxyl group (C═O) of aldehyde or ketone functional group arising for flavonoids and tannins derivatives. The band at 1384 cm^{-1} can be related to the –CH bending vibration of alkane/alkene. Further FT-IR spectra of the extract band at 1203, 896, and 660 cm^{-1} are recognized as a C–O group of aliphatic ester, N–H (1^{o} and 2^{o} amines) respectively. The overall spectral results indicate the leaves extracts presented phytochemicals compounds such as polyphenolic compounds of flavonoids, tannin, and coumarins, which might be involved the reducing and stabilizing the synthesis of NPs.

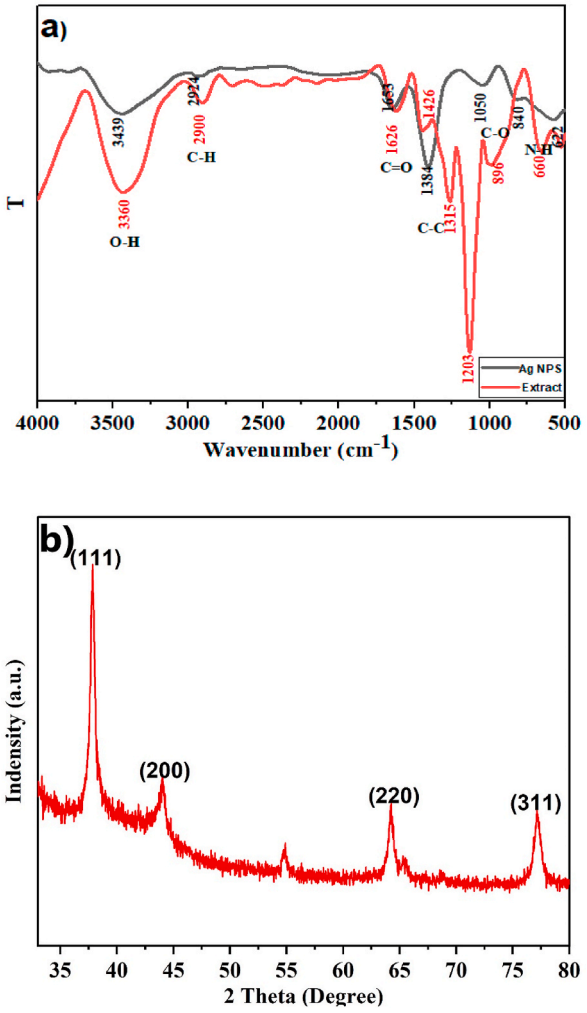

Fig. 2. Green synthesized Ag NPs; a) FTIR Spectrum; b) XRD Spectrum. (For interpretation of the references to colour in this figure legend, the reader is referred to the Web version of this article.)

3.3. XRD analysis

The crystalline nature of Ag NPs was determined the X-ray diffraction (XRD) analysis as shown in Fig. 2b. The different diffraction peaks 2θ values at 37.8°, 44.02°, 64.2°, and 77.1° correspond to the lattice planes at (111), (200), (220), and (311) due to the face-centered-cubic nature of metallic silver and corroborated with JCPDS file No 04–0783. Ondari and Nalini reported similar observations for Ag NPs synthesized using *Tridax procumbens* [33]. The Debye-Scherrer equation was used to determine the average particle size found to be 30–50 nm [34].

3.4. Morphology and sizes of Ag NPs

The valuable information about the size and morphology shape of Ag NPs was identified through the High Resolution Transmission Electron Microscopy (HR TEM) image of synthesized Ag NPs (Fig. 3a&b). The particles were formed in a spherical shape with sizes ranging between 30 and 50 nm in diameter, non-aggregated, and highly dispersed on the surfaces [35]. Moreover, the HR TEM image Fig. 3c shows that the lattice fringe spacing is 0.23 nm. Fig. 3d shows the strong signals observed from the SAED pattern revealed concentric four rings at (111), (200), (220), and (311) were different crystallographic planes of FCC structure of metallic silver. The four-ring of the elemental silver confirmed the XRD analysis. The growth of the Ag NPs is mainly in the (111) plane at 3 keV, through the Energy-Dispersive Spectroscopy (EDS) analysis of Ag NPs Fig. 3e. Which consider as the peak characteristic of metallic Ag NPs is 58.99% by weight, as confirmed by EDS [36]. Other signals originated from carbon and copper were other originated signal that is because of the TEM grid. The graphical representation of the histogram (Fig. 3f) of synthesized Ag NPs has an average particle size, of about 30–50 nm.

3.5. Antimicrobial activity

Many studies have shown the antimicrobial activity of Ag NPs against various pathogenic and multidrug-resistant microorganisms [37]. The antimicrobial activity of *A. marmelos* leaf extract mediated synthesis of Ag NPs showed excellent activity against the

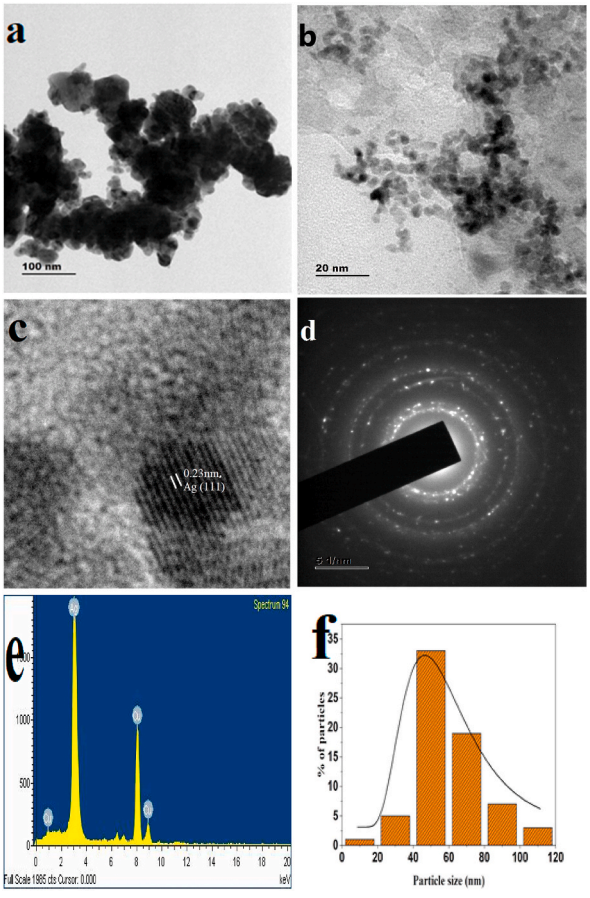

Fig. 3. TEM morphology images of Ag NPs; a) lower magnification image 100 nm; (b) higher magnification 20 nm; (c) Spherically-shaped Ag NPs showing fringe spacing of 0.23 nm; (d) SAED pattern; (e) EDX spectrum; (f) Particle size distribution histogram.

gram-positive and gram-negative pathogens such as *Streptococcus Sp and Klebsiella Sp than Staphylococcus aureus, Pseudomonas aeruginosa*. Different concentrations of Ag NPs (5 μg/mL, 10 μg/mL & 25 μg/mL) were added the respective bacteria as shown in Fig. 4a-d. After 24 h, the zone of inhibition of Ag NPs was measured in mm as shown in Table 1. The antibacterial activity of synthesized Ag NPs was compared with *A. marmelos* extract, control, and standard antibiotic chloramphenicol. The graph result (Fig. 4e) shows the highest zone of inhibition was observed at 25 μg/mL of Ag NPs. In our results clearly indicated that the green synthesized Ag NPs shows effective potential antibacterial activity in the gram positive bacteria compared to gram negative bacteria. Recently, *Ludwigia octovalvis* [38], *Solanum nigrum leaves* [39], *Mimusops elengi* fruit [40] *Salacia chinensis* L [41] extract mediated synthesized Ag NPs was reported the antibacterial activity against the gram negative and gram positive stain. Similarly, the plant extract mediated green synthesized Ag NPs was investigated the antifungal activity against *A. Niger, A. flavus, Candida Sp, and Penicillium Sp* (Fig. 5(a–d)). The zone of inhibition results were interpreted the standard deviation of mean diameter are given in Table 2. All the tested Ag NPs shows strong antifungal activity against *A. Niger, A. flavus, Candida Sp, and Penicillium Sp*. The correct mechanism of the antifungal effect of green synthesized Ag NPs is not determined [42]. The Ag NPs were examining to the superior activity against the extract and standard commercial compound Nystatin. In our results, the synthesized Ag NPs demonstrated highest antifungal activity against *Candida Sp, and Penicillium Sp* (Fig. 5e). This results was corroborate with *Cassia roxburghii* aqueous leaf extract mediated synthesis of Ag NPs shows good antifungal activity against different fungi [43,44].

3.6. Antioxidant activity

Free radicals, which cause destruction and mutation in cells, are dangerous to human health. Antioxidant shows a significant role

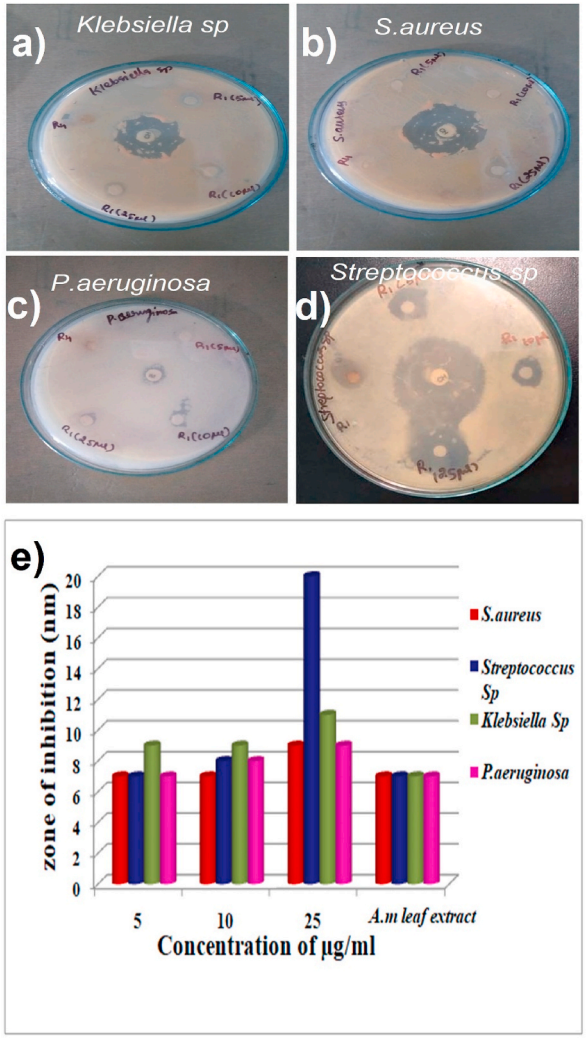

Fig. 4. Well diffusion assay (a–e) to assess the bacterial potential of Ag NPs at three different concentrations 5, 10, 25 μg/mL against various bacterial strains (a) *Klebsiella Species*; (b) *Staphylococcus aureus*; (c) *Pseudomonas aeruginosa*; (d) *streptococcus Species*; (e) Antibacterial Activity.

Table 1
Zone of inhibition (mm) at different concentrations of Ag NPs.

S. No	Name of bacterial species	Zone of Inhibition (nm)			
		5 μg/mL	10 μg/mL	25 μg/mL	*A. marmelos* LE (25 μg/mL)
1	*S.aureus*	7	7	9	7
2	*Streptococcus Sp*	7	8	20	7
3	*Klebsiella Sp*	9	9	11	7
4	*P.aeruginosa*	7	8	9	7

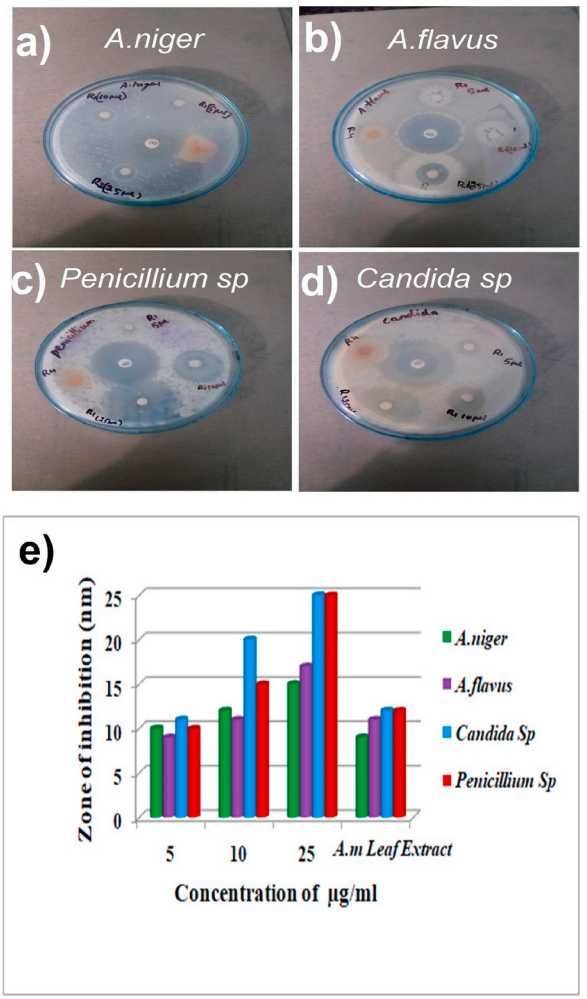

Fig. 5. Well diffusion assay (a–e) to assess the fungal potential of Ag-NPs at three different concentrations 5, 10, 25 μg/mL against various fungal strains (a) *Aspergillus niger*; (b) *Aspergillus flavus*; (c) *Penicillium species*; (d) *Candida Species;* (e) Antifungal Activity.

Table 2
Zone of inhibition (mm) at different concentrations of Ag NPs.

S. No	Name of fungi species	Zone of Inhibition (nm)			
		5 μg/mL	10 μg/mL	25 μg/mL	*A. marmelos* LE (25 μg/mL)
1	*A.niger*	10	12	15	9
2	*A.flavus*	9	11	17	11
3	*Candida Sp*	11	20	25	12
4	*Penicillium Sp*	10	15	25	12

for the scavenging activity. Recently the natural products of phytochemical mediated green synthesized metal nanoparticles have been high antioxidant activity. DPPH free radical scavenging is a well known method to determine the antioxidant activity. In this study, the Ag NPs was added to DPPH at the time the solution measured wavelength absorption at 517 nm. The DPPH scavenging activity has increased with increasing the concentration of Ag NPs and standard ascorbic acid (Fig. 6). The DPPH is a stable free radical compound and can gain electrons from antioxidant molecules. The free radical scavenging activity of Ag NPs showed a maximum of 90% at $IC_{50} = 99.37 \pm 0.36$ μg/mL and a similar concentration of standard ascorbic acid exhibited 80% inhibition at $IC_{50} = 21.54 \pm 1.5$ μg/mL. The main reason is due to the presence of phytochemicals such as proteins, flavonoids, carbohydrates, and phenolic compounds to presence of –OH group. The high hydroxyl groups stabilized Ag NPs has responsible for potential antioxidant activity [45,46].

3.7. Anticancer activity

The synthesized Ag NPs were determined the anticancer (cytotoxicity) activity in the MDA-MB-231 human breast cancer cells using MTT assay. MDA-MB-231 human breast cancer cells were also treated with different concentrations (25, 50, 100, 250, and 500 μg/mL) of synthesized Ag NPs and *A. marmelos* leaf extract for different dose concentrations. After, 24 h the treated cells were examined the changes of nuclear morphology (Fig. 7(a–f)). The cells viability was considerably reduced in the presence of green synthesized Ag NPs as compared with the positive/negative control. At 24 h treatment, the IC_{50} value of the phytoconstituted *A. marmelos* leaf extract was found to be 179.1 ± 5.73 μg/mL and synthesized Ag NPs was observed at 125 ± 4.26 μg/mL respectively. This result shows that the minimum dose of synthesized Ag NPs showed good cytotoxicity activity against the MDA-MB-231 human breast cancer cell line (Fig. 7g). *A. marmelos* leaf extract mediated synthesized Ag NPs have better and lower activity than the cytotoxicity results corroborate of previous reports [14,47–49]. Several studies suggest that the remarkable cytotoxicity (anticancer) of biologically synthesized MNPs was increased with the increasing concentration of NPs [50–53], and which are compared with Ag NPs and results are summarized in Table 3.

3.8. Photocatalytic activity

The photocatalytic degradation effect of Ag NPs was used as Nano catalyst in the degradation of environmentally polluted organic dye of BF dye under direct solar light. The cationic BF dye (Fig. 8a) solution was determined the UV–vis spectrophotometer absorption wavelength shows at 542 nm [54]. By the addition of Ag NPs in the BF dye solution to standby direct solar light, the dark red colour was changes to colourless within 18 min as shown in Fig. 8c (insert image). This colour changes were clearly identify the degradation of dyes [55]. The photocatalyst Ag NPs was added to BF dye solution, the progress of the dyes degradation was periodically monitored in two ways (direct irradiation of solar light and dark place) by UV–vis spectra at different time intervals. The reaction solution was monitored by without irradiation of solar light (dark place) condition, the BF dyes solution wavelength at 547 nm adsorption intensity was gradually decreased up to 70 min (Fig. 8b) indicating the degradation process very slow. Similarly the same BF dyes solution was irradiated direct solar light, the wavelength at 547 nm absorption intensity was gradually decreased the to confirm the degradation of BF dye within 18 min as shown in Fig. 8c. Therefore, the dye degradation process was faster under solar light irradiation than dye degradation in the dark. More electrons are available to oxygen from Ag NPs under solar light irradiation, increasing the reaction process [56]. The percentage of dye degradation calculated using $[(C_0\text{-}C_t)/C_0] \times 100$ is about 93% and 98% in the dark and solar light irradiation respectively and which are compared with Ag NPs and results are summarized in Table 4.

The photocatalytic activity of Ag NPs used BF dye degradation proposed mechanism has shown in Fig. 8d. The BF dye added Ag NPs catalyst was irradiation of solar light and to generate the electrons was easily migrating from valence band to conduction band gap thus time holes was formed in the valence band. In this process time, the photocatalyst of Ag NPs reaction mixture water (H_2O) molecules were oxidized to form hydroxyl radicals (OH^-*) and anionic superoxide radicals (O_2^-) were produced the holes respectively reported [57–59]. The holes were reacted with water or hydroxide (OH^-) ion, which absorbed into the surface of Ag NPs to form hydroxyl (OH*) radicals. All the hydroxyl radicals (OH^-*) and anionic superoxide radicals (O_2^-*) are potential active species in the degradation of environmentally polluted organic BF dye molecules into H_2O and CO_2 molecules [60–62].

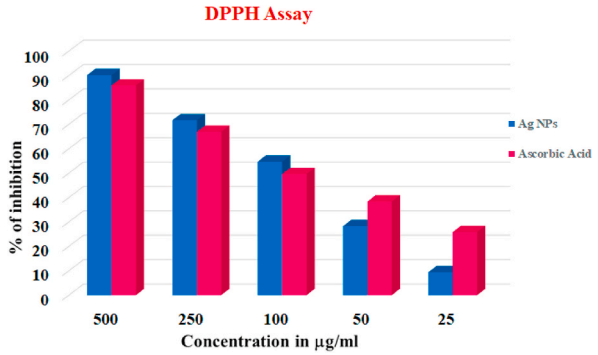

Fig. 6. DPPH assay: Antioxidant activity of Ag NPs.

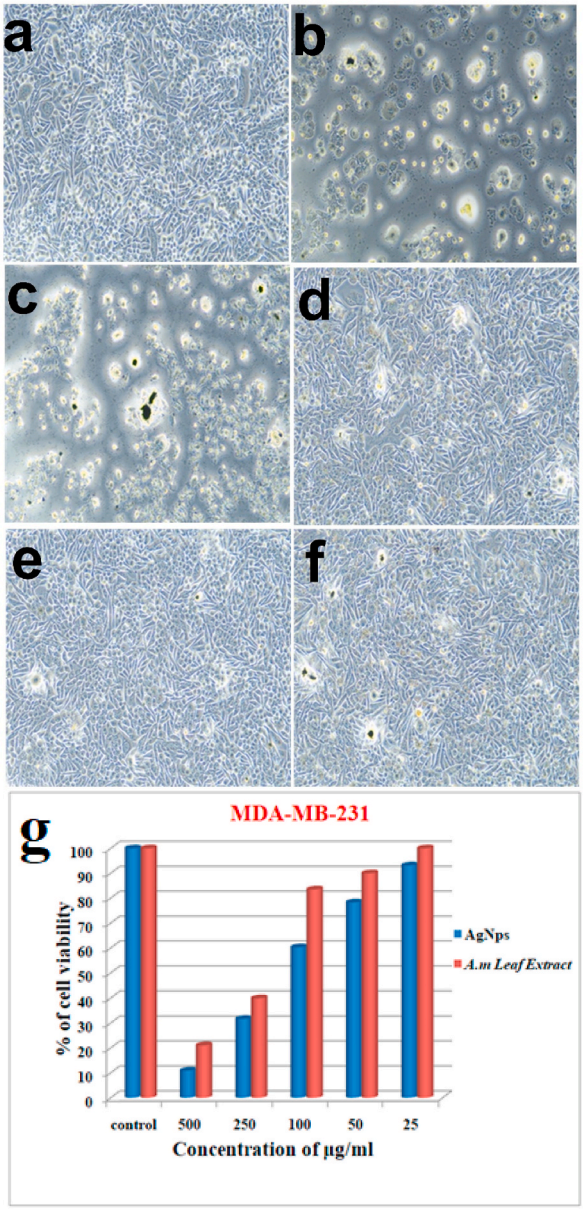

Fig. 7. Anticancer activity of Ag NPs, (a) Control (MDA-MB-231 cells); (b) 500 µg/mL; (c) 250 µg/mL; (d) 100 µg/mL; (e) 50 µg/mL; (f) 25 µg/mL; (g) Cytotoxic activity.

Table 3
Comparative Studies Ag NPs from plants that inhibit the breast cancer cell line MDA-MB-231.

Plant	Part Used	NP Size/NP Shape	IC_{50}	Ref.
Baccaurea ramiflora (Latka)	fruit	10–50 nm/spherical	140 µg/mL	[14]
Gracilaria edulis	marine seaweed	62 nm/spherical	344.27 µg/mL	[48]
Bryophyllam daigremontianum	leaves	Spherical	175.04 µg/mL	[49]
Thymbra	leaf	20 nm/graphene sheets	403 µg/mL	[51]
Prunus nepalensis	fruits	35–50 nm/face centered cubic	158.5 µg/mL	[52]
Baccaurea ramiflora	fruit	10–50 nm/spherical	140 µg/mL	[53]

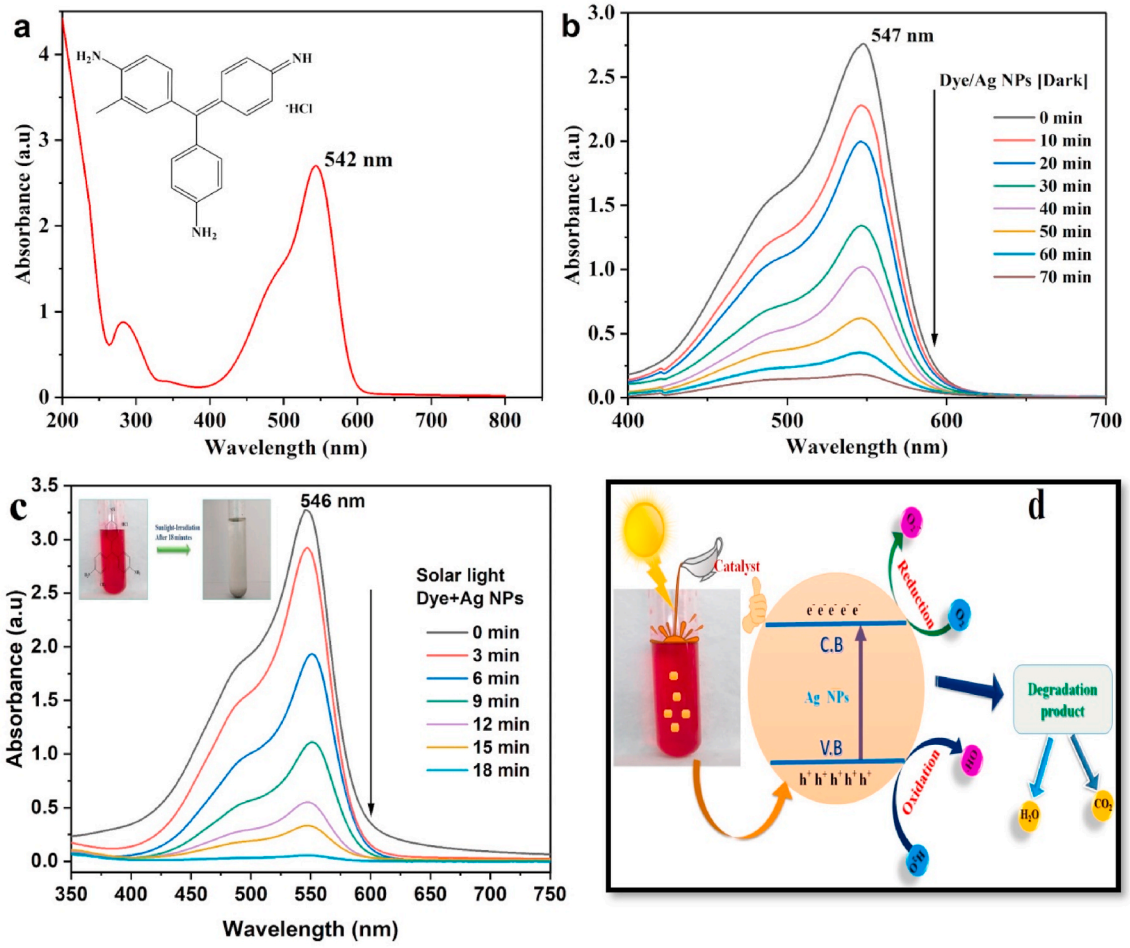

Fig. 8. Photocatalytic degradation of BF dye in the presence of Ag NPs; (a) UV–Vis. spectra and the structure of BF dye; (b) The absorption spectra of FB dye in water in the presence of Ag NPs at different time intervals in the dark irradiation; (c) under Solar light irradiation; (d) Scheme postulated mechanism of photodegradation of BF dye by the aid of Ag NPs.

Table 4
Comparative Studies Ag NPs from plants that the photocatalytic activity of Basic Fuchsin Dye.

Catalyst	Conc. of dye	Conc. of catalyst	Degradation time (min)	Degradation (%)	Refs.
Se NPs	20 mL	10 mg	34 min	100%	[55]
Fe NPs-JF	45.0 mL	50.0 mg	20 min	87.5%	[63]
Graphene Oxide/Zinc Oxide	–	graphitic nano sheet	300 min	92.5%,	[54]
Ag NPs	25 mL	1 mL	18 min	98%	Present work

4. Conclusion

In conclusion, a simple, facile, inexpensive, eco-friendly, and green synthesis of Ag NPs was synthesized from *A. marmelos* in an aqueous medium without employing manmade chemicals. The appearance of dark brown colour and UV–vis. spectral surface Plasmon resonance centre at 450 nm was confirmed the product of Ag NPs. The FT-IR analysis was determine the preliminary phytochemicals of flavonoids, carbohydrates hydroxyl/carbonyl group capped the formation of Ag NPs. HR TEM image showed a spherical shape with an average particle sizes 30–50 nm, whereas the crystalline structure of Ag NPs was observed by the SAED pattern. The presence of silver in the Ag NPs is 58.99% by weight, as confirmed by energy-dispersive X-ray spectroscopy. In this manner, Ag NPs were highly stable and strong antimicrobial and antioxidant activity than the corresponding *A. marmelos* leaf extract. The synthesized Ag NPs possess high anticancer activity against MDA-MB-231 cell lines than the *A. marmelos* leaf extract. Further, the Ag NPs exhibited excellent photo-catalyst in the degradation of BF dye within 18 min for 98%. The present work was contributes the novel and alternative process in the cancer treatment and development of environmentally benign catalyst in the removal of dyes from industrial wastewater management.

Author contribution statement

P. Rama: Conceived and designed the experiments; Performed the experiments; Analyzed and interpreted the data; Wrote the paper.

P. Mariselvi: Analyzed and interpreted the data; Contributed reagents, materials, analysis tools or data; Wrote the paper.

R. Sundaram: Performed the experiments; Analyzed and interpreted the data; Wrote the paper.

K. Muthu: Conceived and designed the experiments; Contributed reagents, materials, analysis tools or data; Wrote the paper.

Data availability statement

Data will be made available on request.

Declaration of competing interest

The authors declare that they have no known competing financial interests or personal relationships that could have appeared to influence the work reported in this paper.

References

[1] F. Bray, J. Ferlay, I. Soerjomataram, R.L. Siegel, L.A. Torre, A. Jemal, Global cancer statistics 2018: globocan estimates of incidence and mortality worldwide for 36 cancers in 185 countries, CA A Cancer J. Clin. 68 (2018) 394–424, https://doi.org/10.3322/caac.21492.

[2] X. Tang, S. Cai, R. Zhang, P. Liu, H. Chen, Y. Zheng, L. Sun, Paclitaxel-loaded nanoparticles of star-shaped cholic acid-core PLA-TPGS copolymer for breast cancer treatment, Nanoscale Res. Lett. 8 (2013) 1–12, https://doi.org/10.1186/1556-276X-8-420.

[3] G. Curigliano, C. Criscitiello, Successes and limitations of targeted cancer therapy in breast cancer, Succes. Limita, Targ. Canc. Ther. 41 (2014) 15–35.

[4] P. Kumari, B. Ghosh, S. Biswas, Nanocarriers for cancer-targeted drug delivery, J. Drug Targ. 24 (2016) 179–191, https://doi.org/10.1159/000355896.

[5] M. Thiruvengadam, G. Rajakumar, I.M. Chung, Nanotechnology: current uses and future applications in the food industry, 3 Biotech. 8 (2018) 1–13, https://doi.org/10.1007/s13205-018-1104-7.

[6] A.K. Mittal, Y. Chisti, U.C. Banerjee, Synthesis of metallic nanoparticles using plant extracts, Biotechnol. Adv. 31 (2013) 346–356, https://doi.org/10.1016/j.biotechadv.2013.01.003.

[7] A. Ebrahiminezhad, M.J. Raee, Z. Manafi, A. Sotoodeh Jahromi, Y. Ghasemi, Ancient and novel forms of silver in medicine and biomedicine, J. Adv. Med. Sci. Appl. Techn. 2 (2016) 122–128, https://doi.org/10.18869/nrip.jamsat.2.1.122.

[8] I.M. Chung, I. Park, K. Seung-Hyun, M. Thiruvengadam, G. Rajakumar, Plant-mediated synthesis of silver nanoparticles: their characteristic properties and therapeutic applications, Nanoscale Res. Lett. 11 (2016) 1–14, https://doi.org/10.1186/s11671-016-1257-4.

[9] P. Kanniah, P. Chelliah, J.R. Thangapandi, G. Gnanadhas, V. Mahendran, M. Robert, Green synthesis of antibacterial and cytotoxic silver nanoparticles by *Piper nigrum* seed extract and development of antibacterial silver based chitosan nanocomposite, Int. J.Biolog. Macromole. 189 (2021) 18–33, https://doi.org/10.1016/j.ijbiomac.2021.08.056.

[10] M.M. Faheem, M. Bhagat, P. Sharma, R. Anand, Induction of p53 mediated mitochondrial apoptosis and cell cycle arrest in human breast cancer cells by plant mediated synthesis of silver nanoparticles from *Bergenia ligulata* (Whole plant), Int. J. Pharmaceutics. 619 (2022), 121710, https://doi.org/10.1016/j.ijpharm.2022.121710.

[11] K. Chitra, M. Sureshkumar, N. Vijayakumar, J.S. Ajarem, A.A. Allam, W. Kim, P. Kumar, Synthesis of silver nanoparticles using *Leucas biflora* (Vahl) Sm. Leaf extracts and their activity on breast cancer (MDA-MB-231) cells, Mater. Lett. 312 (2022), 131706, https://doi.org/10.1016/j.matlet.2022.131706.

[12] S. Sathiyavimal, E.F. Durán-Lara, S. Vasantharaj, M. Saravanan, A. Sabour, M. Alshiekheid, A. Pugazhendhi, Green synthesis of copper oxide nanoparticles using *Abutilon indicum* leaves extract and their evaluation of antibacterial, anticancer in human A549 lung and MDA-MB-231 breast cancer cells, Food Chem. Toxicol. 168 (2022), 113330, https://doi.org/10.1016/j.fct.2022.113330.

[13] Z. Gharari, P. Hanachi, T.R. Walker, Green synthesized Ag-nanoparticles using *Scutellaria multicaulis* stem extract and their selective cytotoxicity against breast cancer, Analy. Biochem. 653 (2022), 114786, https://doi.org/10.1016/j.ab.2022.114786.

[14] S. Banerjee, S. Islam, A. Chattopadhyay, A. Sen, P. Kar, Synthesis of silver nanoparticles using underutilized fruit *Baccaurea ramiflora* (Latka) juice and its biological and cytotoxic efficacy against MCF-7 and MDA-MB 231 cancer cell lines, SouthAfri. J. Botany 145 (2022) 228–235, https://doi.org/10.1016/j.sajb.2021.09.016.

[15] K. Yu, S.G. Yang, C. Liu, H. Chen, H. Li, C. Sun, S.A. Boyd, Degradation of organic dyes via bismuth silver oxide initiated direct oxidation coupled with sodium bismuthate based visible light photocatalysis, Environ. Sci. Technol. 46 (2012) 7318–7326, https://doi.org/10.1021/es3001954.

[16] M. Nasrollahzadeh, M. Atarod, B. Jaleh, M. Gandomirouzbahani, In situ green synthesis of Ag nanoparticles on graphene oxide/TiO_2 nanocomposite and their catalytic activity for the reduction of 4-nitrophenol, Congo red and methylene blue, Ceram. Int. 42 (2016) 8587–8596, https://doi.org/10.1016/j.ceramint.2016.02.088.

[17] S. Singh, V.C. Srivastava, I.D. Mall, Mechanism of dye degradation during electrochemical treatment, J. Phys. Chem. C 117 (29) (2013) 15229–15240, https://doi.org/10.1021/jp405289f.

[18] T. Selvamani, S. Anandan, A.M. Asiri, P. Maruthamuthu, M. Ashokkumar, Preparation of $MgTi_2O_5$ nanoparticles for sonophotocatalytic degradation of triphenylmethane dyes, Ultrason. Sonochem. 75 (2021), 105585, https://doi.org/10.1016/j.ultsonch.2021.105585.

[19] R. Al-Tohamy, S.S. Ali, F. Li, K.M. Okasha, Y.A.-G. Mahmoud, T. Elsamahy, H. Jiao, Y. Fu, J. Sun, A critical review on the treatment of dye-containing wastewater: ecotoxicological and health concerns of textile dyes and possible remediation approaches for environmental safety, Ecotoxicol. Environ. Saf. 231 (2022), 113160, https://doi.org/10.1016/j.ecoenv.2021.113160.

[20] S. Lauren, D. Forge, M. Port, A. Roch, C. Robic, L.V. Elst, R.N. Muller, Magnetic iron oxide nanoparticles: synthesis, stabilization, vectorization, physicochemical characterizations, and biological applications, Chem. Rev. 108 (2008) 2064–2110, https://doi.org/10.1021/cr068445e.

[21] A.V. Nikam, B.L.V. Prasad, A.A. Kulkarni, Wet chemical synthesis of metal oxide nanoparticles: a review, CrystEngComm 20 (2018) 5091–5107, https://doi.org/10.1039/C8CE00487K.

[22] J. Ning, M. Wang, X. Luo, Q. Hu, R. Hou, W. Chen, D. Chen, J. Wang, J. Liu, SiO_2 stabilized magnetic nanoparticles as a highly effective catalyst for the degradation of basic fuchsin in industrial dye wastewaters, Molecules 23 (2018) 2573, https://doi.org/10.3390/molecules23102573.

[23] J. Mhatre, S. Nagaral, S. Kulkarni, Formulation and evaluation of antibacterial activity of a herbal ointment prepared from crude extracts of *Aegle marmelos*, (Bael), Int. J. Pharm. Pharmaceut. Sci. 6 (2014) 575–579. https://www.researchgate.net/publication/267033478_Formulation_and_evaluation_of_antibacterial_activity_of_a_herbal_ointment_prepared_from_crude_extracts_of_Aegle_Marmelos_Bael.

[24] T. Gohil, N. Pathak, N. Jivani, V. Devmurari, J. Patel, Treatment with extracts of *Eugenia jambolana* seed and *Aegle marmelos* leaf extracts prevents hyperglycemia and hyperlipidemia in alloxan induced diabetic rats, Afr. J. Pharm. Pharmacol. 4 (2010) 270–275. https://academicjournals.org/journal/AJPP/article-full-text-pdf/462A3C525706.

[25] S. Rahman, R. Parvin, Therapeutic potential of *Aegle marmelos* (L.)-An overview, Asian Pacif. J. Trop. Dis. 4 (2014) 71–77, https://doi.org/10.1016/S2222-1808(14)60318-2.

[26] S.L. Sukanya, J. Sudisha, P. Hariprasad, S.R. Niranjana, H.S. Prakash, S.K. Fathima, Antimicrobial activity of leaf extracts of Indian medicinal plants against clinical and phytopathogenic bacteria, Afr. J. Biotechnol. 8 (2009) 23. https://www.ajol.info/index.php/ajb/article/view/66376.

[27] K. Muthu, S. Priya, Green synthesis, characterization and catalytic activity of silver nanoparticles using *Cassia auriculata* flower extract separated fraction, Spectrochim. Acta, Part A 179 (2017) 66–72, https://doi.org/10.1016/j.saa.2017.02.024.

[28] C. Perez, Antibiotic assay by agar-well diffusion method, Acta Biol. Med. Exp. 15 (1990) 113–115. https://www.researchgate.net/publication/303960600_An_antibiotic_assay_by_the_agar_well_diffusion_method.

[29] M.S. Blois, Antioxidant determinations by the use of a stable free radical, Nature 181 (1958) 1199–1200, https://doi.org/10.1038/1811199a0.

[30] L. Florento, R. Matias, E. Tuaño, K. Santiago, F. dela Cruz, A. Tuazon, Comparison of cytotoxic activity of anticancer drugs against various human tumor cell lines using in vitro cell-based approach, Int. J. Biomed. Sci. 8 (2012) 76. https://www.ncbi.nlm.nih.gov/pmc/articles/PMC3614850/.

[31] S. Patil, R. Sivaraj, P. Rajiv, R. Venckatesh, R. Seenivasan, Green synthesis of silver nanoparticle from leaf extract of *Aegle marmelos* and evaluation of its antibacterial activity, Int. J. Pharm. Pharmaceut. Sci. 7 (2015) 169–173. https://www.researchgate.net/publication/282198490_Green_synthesis_of_silver_nanoparticle_from_leaf_extract_of_aegle_marmelos_and_evaluation_of_its_antibacterial_activity.

[32] K. Muthu, S. Rini, S.M. Nagasundari, B. Akilandaeaswari, Photocatalytic reduction and antioxidant potential of green synthesized silver nanoparticles from *Catharanthus roseus* flower extract, Inorganic Nano-Metal Chem. 51 (2021) 579–589, https://doi.org/10.1080/24701556.2020.1799404.

[33] O.N. Erick, N.M. Padmanabhan, Antimicrobial activity of biogenic silver nanoparticles synthesized using *Tridax procumbens L*, Int. J. Curr. Res. Aca. Rev 2 (2014) 32–40, in: https://www.researchgate.net/publication/264128940_Antimicrobial_activity_of_biogenic_silver_nanoparticles_synthesized_using_Tridax_procumbens_L.

[34] M. Venkatesham, D. Ayodhya, A. Madhusudhan, G. Veerabhadram, Synthesis of stable silver nanoparticles using *Gum acacia* as reducing and stabilizing agent and study of its microbial properties: a novel green approach, Int. J. Green Nanotechnol. 4 (2012) 199–206, https://doi.org/10.1080/19430892.2012.705999.

[35] A.C. Gomathi, S.X. Rajarathinam, A.M. Sadiq, S. Rajeshkumar, Anticancer activity of silver nanoparticles synthesized using aqueous fruit shell extract of *Tamarindus indica* on MCF-7 human breast cancer cell line, J. Drug Deliv. Sci. Technol. 55 (2020), 101376, https://doi.org/10.1016/j.jddst.2019.101376.

[36] M. Gomathi, P.V. Rajkumar, A. Prakasam, K. Ravichandran, Green synthesis of silver nanoparticles using *Datura stramonium* leaf extract and assessment of their antibacterial activity, Resource-Efficient Technolo 3 (2017) 280–284, https://doi.org/10.1016/j.reffit.2016.12.005.

[37] H.H. Lara, N.V. Ayala-Núnez, L.D.C.I. Turrent, C.R. Padilla, Bactericidal effect of silver nanoparticles against multidrug-resistant bacteria, World J. Microbiol. Biotechnol. 26 (2010) 615–621, https://doi.org/10.1007/s11274-009-0211-3.

[38] D.S. Kannan, S. Mahboob, K.A. Al-Ghanim, P. Venkatachalam, Antibacterial, antibiofilm and photocatalytic activities of biogenic silver nanoparticles from *Ludwigia octovalvis*, J. Clust. Science. 32 (2021) 255–264, https://doi.org/10.1007/s10876-020-01784-w.

[39] U. Jinu, N. Jayalakshmi, A. Sujima Anbu, D. Mahendran, S. Sahi, P. Venkatachalam, Biofabrication of cubic phase silver nanoparticles loaded with phytochemicals from *Solanum nigrum* leaf extracts for potential antibacterial, antibiofilm and antioxidant activities against MDR human pathogens, J. Cluster Sci. 28 (2017) 489–505, https://doi.org/10.1007/s10876-016-1125-5.

[40] N. Korkmaz, Y. Ceylan, A. Hamid, A. Karadağ, A.S. Bülbül, M.N. Aftab, F. Şen, Biogenic silver nanoparticles synthesized via *Mimusops elengi* fruit extract, a study on antibiofilm, antibacterial, and anticancer activities, J. Drug Deliv. Sci. Technol. 59 (2020), 101864, https://doi.org/10.1016/j.jddst.2020.101864.

[41] M.R. Nagesh, N. Kumar, J.M. Khan, M.Z. Ahmed, R. Kavitha, S.J. Kim, N. Vijayakumar, Green synthesis and pharmacological applications of silver nanoparticles using ethanolic extract of *Salacia chinensis* L, J. King Saud Univ. Sci. 34 (2022), 102284, https://doi.org/10.1016/j.jksus.2022.102284.

[42] D. Elangovan, H.B.H. Rahman, R. Dhandapani, V. Palanivel, S. Thangavelu, R. Paramasivam, S. Muthupandian, Coating of wallpaper with green synthesized silver nanoparticles from *Passiflora foetida* fruit and its illustrated antifungal mechanism, Process Biochem. 112 (2022) 177–182, https://doi.org/10.1016/j.procbio.2021.11.027.

[43] P. Balashanmugam, M.D. Balakumaran, R. Murugan, K. Dhanapal, P.T. Kalaichelvan, Phytogenic synthesis of silver nanoparticles, optimization and evaluation of in vitro antifungal activity against human and plant pathogens, Microbiol. Res. 192 (2016) 52–64, https://doi.org/10.1016/j.micres.2016.06.004.

[44] P. Moteriya, H. Padalia, S. Chanda, Characterization, synergistic antibacterial and free radical scavenging efficacy of silver nanoparticles synthesized using *Cassia roxburghii* leaf extract, J. Gen. Eng. Biotech. 15 (2017) 505–513, https://doi.org/10.1016/j.jgeb.2017.06.010.

[45] S. Donga, S. Chanda, Facile green synthesis of silver nanoparticles using *Mangifera indica* seed aqueous extract and its antimicrobial, antioxidant and cytotoxic potential (3-in-1 system), Artificial Cells, Nanomed. Biotechn. 49 (2021) 292–302, https://doi.org/10.1080/21691401.2021.1899193.

[46] W. Zhao, L. Wang, H. Chen, L. Qi, R. Yang, T. Ouyang, L. Ning, Green synthesis, characterization and determination of anti-prostate cancer, cytotoxicity and antioxidant effects of gold nanoparticles synthesized using *Alhagi maurorum*, Inorg. Chem. Commun. 141 (2022), 109525, https://doi.org/10.1016/j.inoche.2022.109525.

[47] Z. Gharari, P. Hanachi, T.R. Walker, Green synthesized Ag-nanoparticles using *Scutellaria multicaulis* stem extract and their selective cytotoxicity against breast cancer, Anal. Biochem. 653 (2022), 114786, https://doi.org/10.1016/j.ab.2022.114786.

[48] Y.K. Mohanta, A.K. Mishra, D. Nayak, B. Patra, A. Bratovcic, S.K. Avula, M. Saravanan, Exploring dose-dependent cytotoxicity profile *of Gracilaria edulis*-mediated green synthesized silver nanoparticles against MDA-MB-231 breast carcinoma, Oxid. Med. Cell. Longev. (2022), 3863138, https://doi.org/10.1155/2022/3863138.

[49] M. Sridharan, P. Kamaraj, J. Arockiaselvi, T. Pushpamalini, P.A. Vivekanand, S.H. Kumar, Synthesis, characterization and evaluation of biosynthesized Cerium oxide nanoparticle for its anticancer activity on breast cancer cell (MCF 7), Mater. Today: Proc. 36 (2021) 914–919, https://doi.org/10.1016/j.matpr.2020.07.031.

[50] C. Krishnaraj, P. Muthukumaran, R. Ramachandran, M.D. Balakumaran, P.T. Kalaichelvan, *Acalypha indica Linn*: biogenic synthesis of silver and gold nanoparticles and their cytotoxic effects against MDA-MB-231, human breast cancer cells, Biotech. Rep. 4 (2014) 42–49, https://doi.org/10.1016/j.btre.2014.08.002.

[51] H. Liu, W. Shi, Y. Luo, G. Cui, X. Kong, L. Han, L. Zhao, Green supported of Au nanoparticles over reduced graphene oxide: investigation of its cytotoxicity, antioxidant and anti-human breast cancer properties, Inorg. Chem. Commun. 134 (2021), 108918, https://doi.org/10.1016/j.inoche.2021.108918.

[52] S.S. Biresaw, P. Taneja, Copper nanoparticles green synthesis and characterization as anticancer potential in breast cancer cells (MCF7) derived from *Prunus nepalensis* phytochemicals, Mater. Today: Proc. 49 (2022) 3501–3509, https://doi.org/10.1016/j.matpr.2021.07.149.

[53] B. Swarnendra, S. Islam, A. Chattopadhyay, A. Sen, P. Kar, Synthesis of silver nanoparticles using underutilized fruit *Baccaurea ramiflora (Latka)* juice and its biological and cytotoxic efficacy against MCF-7 and MDA-MB 231 cancer cell lines, South Afr. J. Bot. 145 (2022) 228–235, https://doi.org/10.1016/j.sajb.2021.09.016.

[54] Z. Durmus, B.Z. Kurt, A. Durmus, Synthesis and characterization of graphene oxide/zinc oxide (GO/ZnO) nanocomposite and its utilization for photocatalytic degradation of basic Fuchsin dye, ChemistrySelect 4 (1) (2019) 271–278, https://doi.org/10.1002/slct.201803635.

[55] B.A. Al Jahdaly, N.S. Al-Radadi, G.M. Eldin, A. Almahri, M.K. Ahmed, K. Shoueir, I. Janowska, Selenium nanoparticles synthesized using an eco-friendly method: dye decolorization from aqueous solutions, cell viability, antioxidant, and antibacterial effectiveness, J. Mater. Res. Technol. 11 (2021) 85–97, https://doi.org/10.1016/j.jmrt.2020.12.098.

[56] X. Chen, Z. Zheng, X. Ke, E. Jaatinen, T. Xie, D. Wang, C. Guo, J. Zhao, H. Zhu, Supported silver nanoparticles as photo catalysts under ultraviolet and visible light irradiation, Green Chem. 12 (2010) 414–441, https://doi.org/10.1039/B921696K.

[57] S. Sathiyavimal, S. Vasantharaj, T. Kaliannan, A. Pugazhendhi, Eco-biocompatibility of chitosan coated biosynthesized copper oxide nanocomposite for enhanced industrial (Azo) dye removal from aqueous solution and antibacterial properties, Carbohydr. Poly. 241 (2020), 116243, https://doi.org/10.1016/j.carbpol.2020.116243.

[58] N.M. Mahmoodi, M. Oveisi, A. Taghizadeh, M. Taghizadeh, Synthesis of pearl necklace like ZIF-8@chitosan/PVA nanofiber with synergistic effect for recycling aqueous dye removal, Carbohydr. Poly. 227 (2020), 115364, https://doi.org/10.1016/j.carbpol.2019.115364.

[59] S.M. Hosseini, M. Shahrousvand, S. Shojaei, H.A. Khonakdar, A. Asefnejad, V. Goodarzi, Preparation of superabsorbent eco-friendly semi-interpenetrating network based on cross-linked poly acrylic acid/xanthan gum/graphene oxide (PAA/XG/GO): characterization and dye removal ability, Int. J. Biol. Macromole. 152 (2020) 884–893, https://doi.org/10.1016/j.ijbiomac.2020.02.082.
[60] T. de Figueiredo Neves, N.B. Dalarme, P.M.M. da Silva, R. Landers, C.S.F. Picone, P. Prediger, Novel magnetic chitosan/quaternary ammonium salt graphene oxide composite applied to dye removal, J. Environ. Chem. Eng. 8 (4) (2020), 103820, https://doi.org/10.1016/j.jece.2020.103820.
[61] M.D. Firouzjaei, F.A. Afkhami, M.R. Esfahani, C.H. Turner, S. Nejati, Experimental and molecular dynamics study on dye removal from water by a graphene oxide copper-metal organic framework nanocomposite, J. Water Process Eng. 34 (2020), 101180, https://doi.org/10.1016/j.jwpe.2020.101180.
[62] J. Bhadra, H. Parangusan, A. Popelka, M. Lehocky, P. Humpolicek, N. Al-Thani, Electrospun Polystyrene/PANI-Ag fibers for organic dye removal and antibacterial application, J. Environ. Chem. Eng. 8 (3) (2020), 103746, https://doi.org/10.1016/j.jece.2020.103746.
[63] R. Jain, S. Mendiratta, L. Kumar, A. Srivastava, Green synthesis of Iron nanoparticles using *Artocarpus heterophyllus* peel extract and their application as a heterogeneous Fenton-like catalyst for the degradation of Fuchsin Basic dye, Curr. Res. Green Sustain. Chem. 4 (2021), 100086, https://doi.org/10.1016/j.crgsc.2021.100086.